**Visible light photocatalytic activity of novel MWCNT-doped ZnO electrospun nanofibers**

# Visible light photocatalytic activity of novel MWCNT doped ZnO electrospun nanofibers

M. Samadi Amin[a], H. A. Shivaee[a], M. Zanetti[b], A. pourjavadi[c], A. Z. Moshfegh[a,d*1]

[a] Institute of Nanoscience and Nanotechnology, Sharif University of Technology, P.O. Box 14588-8969, Tehran, Iran

[b] Dipartimento di Chimica IFM, Universita` di Torino, Via P. Giuria 7, I-10125 Turin, Italy

[c] Department of Chemistry, Sharif University of Technology, P.O. Box 11365-9516, Tehran, Iran

[d] Department of Physics, Sharif University of Technology, P.O. Box 11555-9161, Tehran, Iran

Multi wall carbon nanotube (MWCNT) doped ZnO electrospun nanofibers prepared using Zinc acetate dihydrate, polyvinyl alcohol (PVA) and the surface modified MWCNT as precursors. The nanofibers prepared by precursor electrospinning were annealed at 460 °C in air to produce doped nanofibers. According to scanning electron microscopy observations, diameter of doped composite nanofibers varied from 120 to 300 nm. The presence of MWCNT in nanofibers confirmed by Raman spectroscopy and TGA curve. Thermal behavior of the composite nanofibers was investigated by thermal gravimetric and differential thermal analysis (TGA-DTA). It was revealed a total weight loss of 55% with no variation in mass reduction at temperature above 460°C. Scanning electron microscopy (SEM), X-ray diffractometry (XRD), Fourier transform infrared spectroscopy (FTIR), and UV-Vis diffuse reflectance spectroscopy (DRS) were employed to characterize the nanofibers properties. The analysis of the DRS data

[a,b] * *Corresponding author: moshfegh@sharif.edu*
*Tel: +98-21-6616-4516*
*Fax: +98-21-6601-2983*

showed the energy band gaps were determined as 3.11 and 2.94 eV for pure ZnO and MWCNT doped ZnO nanofibers, respectively. The FTIR spectrum indicates the formation of Zn–O bond at 452 $cm^{-1}$. From XRD data, it was found that the MWCNT doped ZnO nanofibers are crystalline with hexagonal wurtzite structure. The photocatalytic properties of the doped nanofibers showed a better activity for the degradation of methylene blue under both UV and visible light.

## 1. Introduction

Zinc oxide is an n-type semiconductor with a direct wide band gap and large exciton binding energy [1]. Up to date, 1D ZnO nanomaterials have been successfully synthesized by various methods for application in gas sensing [2], dye-sensitized solar cells [3], and photocatalyst [4]. Photocatalytic property of ZnO nanostructures under UV irradiation for degradation of organic pollutants, dye materials, and pesticides has been widely investigated in the last decade. However, the major drawback in practical photocatalytic application of ZnO is that it does not absorb visible light due to its high band gap energy and it is effective under UV illumination. On the other hand, only approximately 4% of solar light contains UV radiation so pure ZnO is not effective for dye degradation under solar radiation. Therefore, the development of photocatalyst that is excited by visible light can overcome this problem. Up to date, various efforts have been attempted to extend the light absorption of the ZnO to the visible region including: ZnO doping by nitrogen converting ZnO from n-type to p-type [5], preparation of $(Ga_{1-x}Zn_x)$ $(N_{1-x}O_x)$ from GaN and ZnO [6], synthesis of ZnO nanoparticles by dc thermal plasma for better anti-bacterial ability in visible light [7], co doping of cadmium and copper leads to $Cd^{2+}$ incorporation into ZnO crystal structure and formation of shallow state below the conduction band [8].

Hybrid of Carbon nanotube (CNT) with inorganic materials reviewed recently [9] and they attracted much attention due to potential application in photocatalyst, gas sensors, supercapacitors, and field emission devices. MWCNT–ZnO represents one of the most important members of the MWCNT–inorganic composites family. Recently, studies indicate that MWCNT–ZnO made by different preparation methods could possess unique properties which are different from MWCNT and ZnO alone. Huang and his co-workers prepared spinous CNT–ZnO composite materials by thermal CVD and investigate the field emission properties [10]. Zhang et al. deposited ZnO nanodots onto CNT films by ultrasonic spray as an electrode for supercapacitor and showed better capacitive properties such as lowest interfacial electron transfer resistance, very high capacitance and good reversibility in the repetitive charge/discharge cycling test [11]. ZnO–CNT 3D hybrids were fabricated by Yan et al, show revisable surface wettability between superhydrophility and superhydrophobity [12]. The enhancement of photocatalytic property of CNT–ZnO prepared by sol-gel method [13], mild hydrothermal conditions [14] and ZnO nanocrystals-coated MWCNTs composite [15] were also studied.

Generally, one dimensional nanostructured materials, especially nanofibers have received considerable attention because of their high surface to volume ratio (A/V) and long axial ratio. These properties are important parameters for catalyst application. Among various nanofiber synthesis methods [16], electrospinning is a relatively simple and inexpensive top-down method for fabricating a variety of non-woven nanofibers [17-20]. In order to enhance the physical and chemical properties of the electrospun nanofibers, doping with selected elements is an effective method. Doped ZnO electrospun nanofibers with different metals and salts have been studied in

recent years and the results show that the properties of doped ZnO nanofibers improved as compared with pure ZnO electrospun nanofibers [21-24].

The main goal of this study is to demonstrate that electrospinning, as an easily accessible method, could be successfully employed to fabricate MWCNT doped ZnO composite Nanofibers for photocatalytic activity under visible light. To the best of our knowledge, there is no previous report on it. The produced nanofibers are characterized using a variety of analytical methods, including raman spectroscopy, thermal gravimetric and differential thermal analysis (TGA-DTA), field emission scanning electron microscopy (FE-SEM), X-ray diffraction (XRD), X-ray photoelectron spectroscopy (XPS), Fourier transform infrared spectroscopy (FTIR), ultraviolet–visible (UV–Vis) spectrophotometry, and photoluminescence spectroscopy. Subsequently, the photocatalytic activity of both pure ZnO and MWCNT doped nanofibers was evaluated by measuring the photo-degradation of methylene blue under the ultraviolet and visible photo irradiation.

## 2. Experimental Procedure

### 2.1. Fabrication of pure ZnO and MWCNT doped ZnO nanofibers

In order to prepare MWCNT doped ZnO nanofibers, first, Pristine MWCNT (Diameter: 20-70 nm and Length: dozen micron) from Nano Carbon Technologies Company (Akishima-Shi, Tokyo, Japan) were oxidized in a mixture of concentrated sulfuric and nitric acids (3:1, 98% and 69%, respectively, Sigma) at 50 $^{\circ}$C for 6 h. Then the mixture was neutralized with sodium hydroxide solution and the solution of oxidized MWCNTs was vacuum-filtered. The filtered solid washed with deionized water and finally, the oxidized MWCNTs were dried in oven for 24 h at 100 $^{\circ}$C. For preparation of MWCNT doped ZnO nanofibers by electrospinning, PVA with

molecular weight 75,000 and zinc acetate dihydrate ($(CH_3CO_2)_2Zn.2H_2O$) and oxidized MWCNT were used as the precursor materials. First, the 0.03 g MWCNT was dispersed in 4.5 mL distilled water by ultra-sonication for 90 min and then 0.5 g PVA added to it, followed by constant stirring for 60 min at 65 °C. Then, 1 g zinc acetate was added to the PVA and MWCNT solution with constant stirring for 100 min at about 80 °C to obtain a homogenous solution. Same procedure was used to prepare pure ZnO nanofibers precursor without using of MWCNT.

The solution was loaded into a plastic syringe with a 0.7 mm diameter stainless steel needle in horizontal direction respect to collector. A positive voltage 9 kV was applied to the needle while the metal collector was at negative voltage. The feeding rate of the solution was adjusted at a constant rate of a 0.4 mL/h. The distance between the tip of the syringe needle and the rotating drum collector was fixed at 12 cm. The electrospun nanofibers were distributed uniformly over aluminum foil that had been placed on the rotating drum and then as spun nanofibers were calcinated at 460 °C in air with a heating rate of 4 °C/min for 2 hours.

**2.2. Characterization**

Surface morphology of nanofibers was studied by field-emission scanning electron microscopy (S4160 Hitachi). The phase and crystallinity of the nanofibers were characterized using X-ray diffractometer (PW 3710 Philips) with Cu Kα radiation (λ=1.54056 °A). Raman spectroscopy with a 1532 nm Nd YAG laser (LABRAM 800 HR) were used to study the structure of MWCNT doped ZnO nanofibers. Thermal gravimetric and differential thermal analysis (Rheometric Scientific STA1500) was used to determine the calcination temperature of the as spun fibers. Measurements were conducted from 25 to 800 °C, using a heating rate of 10 °C/min in air atmosphere. UV-Visible diffuse reflectance spectrum was recorded on AVA light

DH-S Spec 2048 spectrophotometer. FTIR spectra were recorded on a Perkin Elmer Spectrum RXI for determining bond position in nanofibers. Photoluminescence spectroscopy (Varian Cary Eclipse Fluorescence Spectrophotometer) is used for showing electrons and holes recombination.

### 2.3. Photocatalytic activity measurement

The photocatalytic activity of MWCNT doped ZnO nanofibers was examined using methylene blue (MB) degradation in aqueous solution under both UV and visible light irradiation. In dye degradation investigations by UV irradiation, the experiments were carried out in 50 mL beaker charged with 20 mL of $10^{-5}$ M MB and 10 mg of nanofibers. Prior to irradiation, the mixture solution was kept in a dark place for 60 min to obtain adsorption–desorption equilibrium and the concentration of the solution was determined as initial concentration ($C_0$) of the dye solution. A UV lamp 15 W was placed at about 7 cm above the dye solution and illuminate to sample for 120 min. Then a few milliliters of solution were drawn from the reaction mixture by syringe and loaded in a UV–Vis spectrophotometer (Perkin Eelmer Lambda 950).

Degradation of dye under visible light was carried out by solar simulator (Luzchem's SolSim) and using 10 mL of $10^{-5}$ M dye and 3 mg nanofibers. Poly carbonate filter is used to eliminate any irradiation in UV region. The solution kept in a dark place for 60 min and then illuminated by the power of 80 lux, and the distance between solar source and sample was 18 cm.

## 3. Results and discussion

### 3.1. Scanning electron microscopy

Figure 1 illustrates a typical FE-SEM image of the as spun nanofiber PVA/zinc acetate and PVA/zinc acetate/MWCNT before calcination. As can be seen they are smooth without

presence of beads and aggregated MWCNT on the nanofibers compare to MWCNT-$TiO_2$ electrospun fibers [25]. The diameters of the as spun fibers were in the range of 125-500 nm and 250-750 nm for the fibers without and with MWCNT, respectively. The diameters of the calcinated fibers reduced to the 80-200 nm range and 120-300 nm for ZnO and MWCNT doped ZnO nanofibers, respectively(figure 1(c,d)). The diameter reduction of the nanofibers after calcination is due to the decomposition of PVA and the acetate group.

### 3.2. Raman spectroscopy

Raman spectroscopy analysis has been conducted on functionalized MWCNT and MWCNT doped ZnO nanofibers for confirmation the presence of MWCNT in ZnO nanofibers as shown in Figure 2. The Raman spectra of functionalized MWCNT show a G band at about 1582 $cm^{-1}$ and at 1579 $cm^{-1}$ for MWCNT doped ZnO nanofibers that is corresponding to the $E_{2g}$ tangential stretching mode of an ordered graphitic structure with $sp^2$ hybridization and a D band at about 1351 $cm^{-1}$ for functionalized MWCNT and 1342 $cm^{-1}$ for MWCNT doped ZnO nanofibers that is originating from disordered carbon. The origin of this disorder band in the samples is due to the defects in the nano tube wall created after oxidation by acid treatment [26]. Therefore, the intensity ratio of the D over the G peak (ID/IG) band can be used to evaluate the degree of disorder in the walls of the MWCNTs. The D to G band intensity ratio for functionalized MWCNT is 0.53, which is greater than that of the MWCNT doped ZnO nanofibers (about 0.48). The peaks at 2760 $cm^{-1}$ for functionalized MWCNT and at 2698 $cm^{-1}$ is known as the $G'$ band. This is one of the important bands in the CNTs which give information about the stress on the CNTs. Here, there is a down shift in the $G'$ band after electrospinning that could be because of stretching of MWCNT and slight residual tension in it [27]. This result reveals that the

electrospinning method shifts the G and D band of MWCNT and decreases the degree of disorder of the MWCNTs [28].

### 3.3. Thermal analysis

In order to confirm the loading of MWCNT in nanofibers, thermograviametric analysis of the fibers were carried out. This technique was also carried out to determine the decomposition temperature of the precursor and the suitable calcination temperature of the as spun nanofibers. It is evident from TGA curve of pure ZnO and MWCNT doped ZnO nanofibers in figure 3 that most of the organic belonged to PVA and $CH_3COOH$ group of zinc acetate are removed at temperature below 460 $^{\circ}$C in both samples. The difference of the remaining weight between these two samples (35.6% for pure ZnO and 45.1% for MWCNT doped ZnO) at the plateau region at 460 $^{\circ}$C is due to the MWCNT contents. Therefore, the MWCNT content in the nanofibers is about 10 wt %. In the DTA curve of MWCNT doped ZnO, there are three exothermic peaks at about 270, 370 and 450 $^{\circ}$C, probably related to the decomposition of side chain and main chain of PVA and zinc acetate [29]. The weight losses observed in the TGA graph are well matched with the decomposition behavior in the DTA curve. It worth to note, there were no change in weight loss at above 460 $^{\circ}$C, revealing that the calcination temperature at above 460 $^{\circ}$C is needed to remove the solvent and polymer as well as full decomposition of the zinc acetate into pure ZnO phase.

### 3.4. X-ray diffraction

The XRD results for the ZnO and MWCNT doped ZnO nanofibers are presented in figure 4. From the XRD spectra, seven diffraction peaks corresponding to (1 0 0), (0 0 2), (1 0 1), (1 0 2), (1 1 0), (1 0 3) and (1 1 2) planes were present, indicating formation of wurtzite type

structure after MWCNT doping, according to JCPDS card No. 36-1451. In comparison with the spectrum of pure ZnO nanofibers, the intensity of diffraction peaks of MWCNT doped ZnO fibers decreased, indicating that the degree of crystallinity of pure ZnO fibers were better than MWCNT doped ZnO fibers. Furthermore, the full width at half maximum (FWHM) of the MWCNT doped ZnO peaks became larger as compared with pure ZnO peaks. It suggested that the grain size became smaller in ZnO doped nanofibers than in pure ZnO nanofibers as was also seen by others [30, 31]. The lattice constants for MWCNT doped ZnO and pure ZnO nanofibers were found to be a = 3.252 Å, c = 5.211 Å and a = 3.248 Å, c = 5.211 Å respectively, using (100) and (002) peaks.

### 3.5. Fourier transform infrared spectroscopy

The formation of ZnO wurtzite structure in the ZnO and MWCNT doped ZnO nanofibers in the range of 4000–400 $cm^{-1}$ wave number, after calcination at 460°C, was further supported by FTIR spectra, as shown in figure 5. In FTIR spectrum of ZnO nanofibers, There are two bands with very low intensity at 3408 and 2340 $cm^{-1}$ corresponding to the $H_2O$ and $CO_2$ that adsorbed on the surface of the samples. The band at 432 $cm^{-1}$ is due to the Zn–O stretching mode, which indicates the formation of ZnO crystal. The peaks are in the approximately same position in MWCNT doped ZnO nanofiber but the Zn–O peak at 452 $cm^{-1}$ is slightly shifted due to the effect of doping [32]. No peaks corresponding to the functionalized MWCNT in the nanofibers are observed, which may be due to the low MWCNT concentration in the samples.

### 3.6. Ultraviolet-visible spectroscopy

The inset of figure 6 depicts the absorbance data for the pure and MWCNT doped ZnO nanofibers. WMCNT doped ZnO nanofibers revealed a higher absorbance in visible region as

compared to Pure ZnO nanofibers. The band gap energies of nanofibers were calculated from $(\alpha h\nu)^2$ vs. $h\nu$ plot, where α is the optical absorption coefficient from the absorption data of DRS (inset of figure 6) and $h\nu$ is the energy of incident photon. The band gap energy ($E_g$) was estimated by assuming a direct transition between valence and conduction bands from the following expression [33]:

$$\alpha h\nu = K\left(h\nu - \mathrm{E_g}\right)^{1/2}$$

where *K* is a constant and the intercepts of these plots afford an estimate of the optical band gap energy of the corresponding samples as shown in figure 6. A value of 3.11 eV is obtained for pure ZnO nanofibers while the corresponding value for the CNT doped sample is 2.94 eV. Interestingly enough, the $E_g$ value of the doped ZnO is lower than that pure sample. This can be due to the formation Zn-C and Zn-O-C bonds between functionalized MWCNT and ZnO [34, 35]. A similar result was also reported by Akhavan et al. [36] for CNT doped TiO2.

### 3.7. Photocatalytic activity

Methylene blue (MB) has often been used as a model dye molecule for photocatalytic degradation examination of semiconductors. The photocatalytic activity of pure ZnO and MWCNT doped ZnO nanofibers were evaluated by the photocatalytic decomposition of MB dye under the irradiation of UV lights. It is well established that the photocatalytic degradation of MB is classified as the first-order kinetics defined by the following equation:

$\mathrm{Ln}(C/Co) = -kt$

where $C_0$ and C are the concentrations of the MB at $t = 0$ and at later time of *t*, respectively. In this research, the quantity $-\mathrm{Ln}(C/C_0)$ was plotted as a function of the UV-irradiation time for

different samples (figure 7). A linear behavior is observed for samples and the results obey this kinetics. According to the above experimental data analysis, the reaction rate constants (k) from the slop of the linear fit were 0.00286 $min^{-1}$ for pure ZnO nanofibers and 0.01445 $min^{-1}$ for MWCNT doped ZnO nanofibers. It is obvious that the rate of MB degradation by MWCNT doped nanofiber is seven times more than pure nanofibers under UV illumination. As discussed in section 3.4 the grains size of the MWCNT doped ZnO nanofiber are smaller than the pure ZnO nanofibers, on the other hand as depicted in FE-SEM image the diameter of the doped nanofibers is more than pure one. Therefore, the surface area of the MWCNT doped nanofiber is more than pure one that resulted in higher MB absorption and enhanced photo-degradation reaction of dye molecule on the surface of the MWCNT doped ZnO nanofibers. In addition to the difference in surface area of both nanofibers, the presence of MWCNT may cause the retardation of electron ($e^-$) and hole ($h^+$) recombination process and this is confirmed by PL spectrum [37]. Figure 8 shows the emission band at 520 nm for MWCNT doped ZnO and pure ZnO nanofibers. The PL intensity of the pure nanofibers is more than doped one, and the reduction of PL intensity indicates the decrease of radiative recombination process. Thus, the presence of MWCNTs in nanofibers is detrimental in delaying $e^-$–$h^+$ recombination process under UV light. Proposed mechanism for enhancing photocatalytic properties under UV illumination of $TiO_2$-CNT by Woan et al. [38] is shown in figure 10. In MWCNT doped ZnO nanofibers, photogenerated electrons by ZnO after UV irradiation may move freely toward the MWCNT surface and holes remain in ZnO valance band. Therefore, the possibility of $e^-$–$h^+$ pair recombination is reduced and as a result the photocatalytic activity of MB degradation is enhanced under UV light. The inset of Figure 7 depicts the UV-Vis spectrum of MB solution of both nanofibers after keeping in a dark place for 60 min using a calibration height of 664 nm for

methylene blue characteristic peak. It is obvious that the MB absorbed on the surface of MWCNT doped ZnO more than of pure ZnO nanofibers, and the height of the peak reduced about 24% as compared to the absorption peak of the dye. This may be due to the oxidation of MWCNT and the presence of surface alcohol, keton and acid groups.

The plot of $-Ln(C/C_0)$ vs. time of MB photodegradation by MWCNT doped ZnO is depicted in figure 10. The MB degradation rate constant from the linear fit of the data is 0.00387 $min^{-1}$ for MWCNT doped ZnO nanofibers The pure ZnO nanofibers had no effect on MB degradation under visible light. From the DRS optical results, the band gap energy is narrowed but the doped samples are not excited by the visible light. The mechanism that suggested by Wang et al. [39] in figure 9 (b) for photocatalytic activity of $TiO_2$-CNT under visible light, proposed that MWCNT is acting as photosensitizer. Here, MWCNT may absorb the visible irradiation and transfer the photogenerated electron into the conduction band of the ZnO and the dye degrade on the surface of the ZnO and the positively charged CNTs remove an electron from the valence band of the ZNO and leaving a hole.

## 4. Conclusions

MWCNT doped ZnO nanofiber were synthesized by electrospinning of the PVA/zinc acetate/oxidize MWCNT precursors and subsequent calcination at 460 $^{\circ}C$. The diameter of the nanofibers was found to vary between 120 and 300 nm. FTIR analysis showed a sharp and strong peak at 452 $cm^{-1}$ indicating the formation of Zn–O bond. The hexagonal wurtzite structure was not changed by the addition of MWCNT, but the transmittance of MWCNT doped ZnO nanofiber is reduced upon the addition of MWCNT and the band gap energy shifted from 3.11 to 2.94. Photocatalytic activity of MB degradation was investigated in both UV and visible light.

The MWCNT doped nanofibers showed a better MB degradation rate under UV irradiation as compared to pure ZnO nanofibers. The pure nanofibers have no activity in visible light, while the MWCNT doped nanofibers degraded about 50% of the MB solution. Since the electrospinning is relatively simple and inexpensive method for successful preparation of MWCNT doped ZnO nanofibers, we believe that these nanostructures could be utilized in numerous applications and especially for degradation of organic pollutants.

**Acknowledgments**

.

The authors wish to thank Research and Technology Council of the Sharif University of Technology for financial support. Useful discussion with Dr. P. Bracco, Dr. R. Azimirad, Dr. O. Moradlou, Dr. R. Ghasempour and Mrs. N. Naseri are greatly acknowledged.

**References**

[1] Zhong Lin Wang, ACS Nano, VOL. 2 ▪ NO. 10 ▪ 1987–1992 ▪ 2008.

[2] Zhenyi Zhang, Xinghua Li, Changhua Wang, Liming Wei, Yichun Liu, and Changlu Shao* *J. Phys. Chem. C* 2009, *113,* 19397–19403

**ZnO Hollow Nanofibers: Fabrication from Facile Single Capillary Electrospinning and Applications in Gas Sensors**

[3] Zhifeng Liu, Chengcheng Liu, Jing Ya, E. Lei Renewable Energy 36 (2011) 1177e1181

**Controlled synthesis of ZnO and TiO2 nanotubes by chemical method and their application in dye-sensitized solar cells**

[4] Min Wang, GuangTao Fei and Li De Zhang *Nanoscale Research Letters* 2010, 5:1800-1803

Porous-ZnO-Nanobelt Film as Recyclable Photocatalysts with Enhanced Photocatalytic Activity

[5] 9 Chen Shifu, ZhaoWei, Zhang Sujuan, LiuWei Chemical Engineering Journal 148 (2009) 263–269.

**Preparation, characterization and photocatalytic activity of N-containing ZnO powder**[6] Kazuhiko Maeda and Kazunari Domen Chem. Mater. 2010, 22, 612–623

**Solid Solution of GaN and ZnO as a Stable Photocatalyst for Overall Water Splitting under Visible Light**

[7] Hsiu-Fen Lin ∗, Shih-Chieh Liao, Sung-Wei Hung Journal of Photochemistry and Photobiology A: Chemistry 174 (2005) 82–87

**The dc thermal plasma synthesis of ZnO nanoparticles for visible-light photocatalyst**

[8] Srinivasan Anandana, Naoki Ohashib, Masahiro Miyauchia,∗ Applied Catalysis B: Environmental 100 (2010) 502–509

**ZnO-based visible-light photocatalyst: Band-gap engineering and multi-electron reduction by co-catalyst**

[9] Dominik Eder *Chem. Rev.* 2010, *110,* 1348–1385.

**Carbon Nanotube-Inorganic Hybrids**

[10] Chien-Sheng Huang, Chun-Yu Yeh, Yung-Huang Chang, Yi-Min Hsieh, Chien-Yeh Ku, Quan-Ting Lai Diamond & Related Materials 18 (2009) 452–456

**Field emission properties of CNT–ZnO composite materials**

[11] Yanping Zhang, Xiaowei Sun, Likun Pan , Haibo Li, Zhuo Sun, Changqing Sun, Beng Kang Tay Solid State Ionics 180 (2009) 1525–1528

**Carbon nanotube–ZnO nanocomposite electrodes for supercapacitors**

[12] Xing-bin Yan, Beng-kang Tay, Yi Yang, and Wendy Yung Ka Po *J. Phys. Chem. C* 2007, *111,* 17254-17259

**Fabrication of Three-Dimensional ZnO-Carbon Nanotube (CNT) Hybrids Using Self-Assembled CNT Micropatterns as Framework**

[13]WANG, Xuejing YAO, Shuwen LI, Xiaobo *Chinese Journal of Chemistry*, 2009, *27*, 1317—1320.

**Sol-gel Preparation of CNT/ZnO Nanocomposite and Its Photocatalytic Property**

[14] K. Byrappa, A. S. Dayananda, C. P. Sajan, B. Basavalingu,

M. B. Shayan, K. Soga, M. Yoshimura J Mater Sci (2008) 43:2348–2355

**Hydrothermal preparation of ZnO:CNT and TiO2:CNT composites and their photocatalytic applications**

[15] Linqin Jiang, Lian Gao Materials Chemistry and Physics 91 (2005) 313–316

**Fabrication and characterization of ZnO-coated multi-walled carbon nanotubes with enhanced photocatalytic activity**

[16] **An introduction to electrospinning and nanofibers,** By Seeram Ramakrishna, Published by World Scientific Publishing Co. 2005

[17] K. Jayaraman, M. Kotaki, Y. Zhang, X. Mo, S. Ramakrishna, J. Nanosci. Nanotechnol. 4 (2004) 52.

[18] D. Li, Y. Xia, Adv. Mater. 16 (2004) 1151.

[19] A. Frenot, I.S. Chronakis, Current Opinion in Colloid and Interface Science 8 (2003).

[20] A. Greiner, J.H. Wendorff, Angw. Chem. Int. Ed. 46 (2007) 5670-5703.

[21] Qi Qi, Tong Zhanga,b, ShujuanWang, Xuejun Zheng Humidity sensing properties of KCl-doped ZnO nanofibers with super-rapid response and recovery Sensors and Actuators B 137 (2009) 649–655

[22] Minggang Zhao, Xinchang Wang, Lingling Ning, Jianfeng Jia, Xinjian Li, Liangliang Cao **Electrospun Cu-doped ZnO nanofibers for H2S sensing Sensors and Actuators B 156 (2011) 588– 592**

[23] Sining Yun a,n, SangwooLim **Improved conversion efficiency in dye-sensitized solar cells based on electrospun Al-doped ZnO nanofiber electrodes prepared by seed layer treatment.** Journal of Solid State Chemistry 184 (2011) 273–279

[24] Minggang Zhaoa, Xinchang Wanga,∗, Lingling Ninga, Hao Hea, Jianfeng Jia a, Liwei Zhangb,c, Xinjian Li, **Synthesis and optical properties of Mg-doped ZnO nanofibers prepared by Electrospinning** Journal of Alloys and Compounds 507 (2010) 97–100

[25] Santosh Aryal a, Chul Ki Kim b, Kwan-Woo Kim c, Myung Seob Khil b, Hak Yong Kim Materials Science and Engineering C 28 (2008) 75–79
**Multi-walled carbon nanotubes/TiO2 composite nanofiber by electrospinning**

[26] Hirsch A 2002 *Angew. Chem. Int. Ed.* 41 1853

**Functionalization of Single-Walled Carbon Nanotubes**

[27] Libo Deng, Stephen J. Eichhorn,Chih-Chuan Kao,and Robert J. Young, ACS Appl. Mater. Interfaces 2011, 3, 433–440

**The Effective Young's Modulus of Carbon Nanotubes in Composites**

[28] Frank Ko, Yury Gogotsi, Ashraf Ali, Nevin Naguib, Haihui Ye, Guoliang Yang, Christopher Li, Peter Willis, Advanced Material, 2003, 15, No 14, 1161-1165

**Electrospinning of continuous carbon nanotube filled nanofiber yarn**

[29] Yanfang Wang, Junhu Zhang, Xiaolu Chen, Xiao Li, Zhiqiang Sun, Kai Zhang, Dayang Wang, Bai Yang, Journal of Colloid and Interface Science 322 (2008) 327–332

[30] Jiaguo Yu, Tingting Ma and Shengwei Liu Phys. Chem. Chem. Phys., 2011, 13, 3491–3501
**Enhanced photocatalytic activity of mesoporous TiO2 aggregates by embedding carbon nanotubes as electron-transfer channelw**

[31] Yanxia Liu, Hongliang Zhang, Xiuyun An, Caitian Gao, Zhenxing Zhang, Jinyuan Zhou, Ming Zhou, Erqing Xie Journal of Alloys and Compounds 506 (2010) 772–776

**Effect of Al doping on the visible photoluminescence of ZnO nanofibers**

[32] Bin Zhou,Youshi Wu, Lili Wu,Ke Zou, Hongde Gai , **Effects of Al dopants on the microstructures and optical properties of ZnO nanofibers prepared by electrospinning** Physica E 41 (2009) 705–710

[33] J. Tauc, R. Grigorovici, and A. Vancu, *Phys. Status Solidi*, 15, 627 (1966)

[34] Tawfik A Saleh, M A Gonda and Q A Drmosh Nanotechnology 21 (2010) 495705 (8pp)
**Preparation of a MWCNT/ZnO nanocomposite and its photocatalytic activity for the removal of cyanide from water using a laser**

[35] Sathyajith Ravindran1 and Cengiz S Ozkan2 Nanotechnology 16 (2005) 1130–1136
**Self-assembly of ZnO nanoparticles to electrostatic coordination sites of functionalized carbon nanotubes**

[36] O. Akhavan,ab R. Azimirad,*c S. Safad and M. M. Larijani J. Mater. Chem., 2010, 20, 7386–7392
**Visible light photo-induced antibacterial activity of CNT–doped TiO2 thin films with various CNT contents**

[37] Ying Yu a,c, Jimmy C. Yu b,d, Cho-Yin Chan a, Yan-Ke Che e, Jin-Cai Zhao e, Lu Ding f, Wei-Kun Ge f, Po-Keung Wong a,d,* Applied Catalysis B: Environmental 61 (2005) 1–11

**Enhancement of adsorption and photocatalytic activity of TiO2 by using carbon nanotubes for the treatment of azo dye**

[38] Woan K, Pyrgiotakis G, Sigmund W. **Photocatalytic carbonnanotube-TiO2 composites**. Adv Mater 2009;21(21):2233–9

[39] Wang W, Serp P, Kalck P, Faria JL. **Visible light photodegradation of phenol on MWNT-TiO2 composite catalysts prepared by a modified sol–gel method.** J Mol Catal A: Chem 2005;235(1–2):194–9.

## Figure captions

### Legends to the Figures:

**Figure 1.** (a)FE-SEM images of pure (a) and MWCNT doped (b) ZnO nanofibers before calcination; pure (c) and MWCNT doped (d) ZnO nanofibers after calcination.

**Figure 2.** Raman spectrum of pure and MWCNT doped ZnO nanofibers.

**Figure 3.** TGA-DTA of the as spun nanofibers with MWCNT dopant.

**Figure 4.** XRD patterns of pure and MWCNT doped ZnO nanofibers.

**Figure 5.** FTIR spectrum of pure and MWCNT doped ZnO nanofibers.

**Figure 6.** Plot of variation of $(\alpha h\nu)^2$ *vs* $h\nu$ for pure and MWCNT doped ZnO nanofibers and UV-Vis spectra of pure and MWCNT doped ZnO nanofibers (inset).

**Figure 7.** Variation of Ln(C/C0) vs. photo-irradiation time under UV light on the pure and MWCNT doped ZnO nanofibers and MB absorption spectra of: Dye solution; Pure ZnO nanofibers; and MWCNT doped nanofibers after keeping in dark for 60 min (inset).

**Figure 8.** Photoluminescence (PL) spectra pure and MWCNT doped ZnO nanofibers

**Figure 9.** MWCNT inhibition of recombination $e^-/h^+$ mechanism in the MWCNT doped ZnO nanofibers under UV light (a) and Photosensitized mechanism of MWCNT in the MWCNT doped ZnO nanofibers (b).

**Figure 10.** Variation of Ln(C/C0) vs. photo-irradiation time under visible light on the MWCNT doped ZnO nanofibers.

**Figure 1**

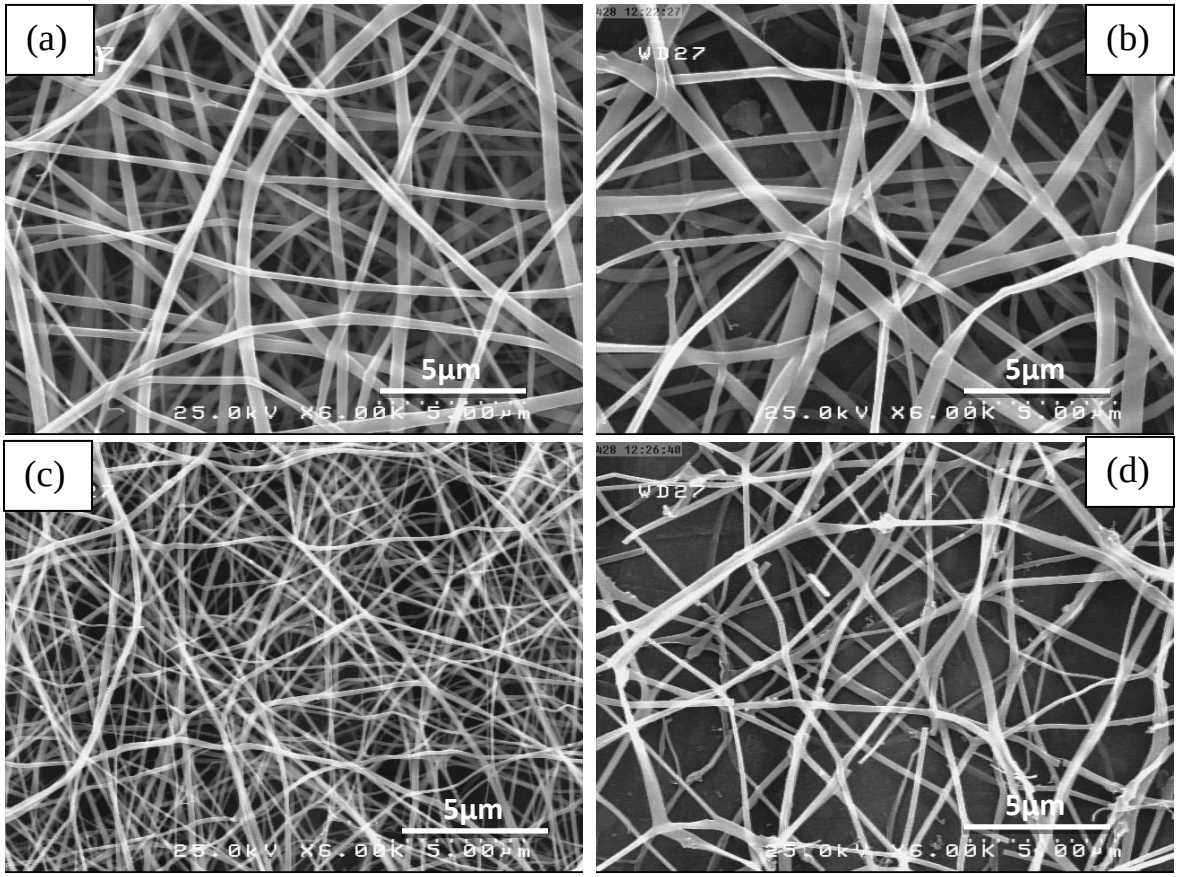
(a)
5µm
25.0kV X6.00K 5.00µm
(b)
WD27
5µm
25.0kV X6.00K 5.00µm
(c)
5µm
25.0kV X6.00K 5.00µm
(d)
WD27
5µm

**Figure 2**

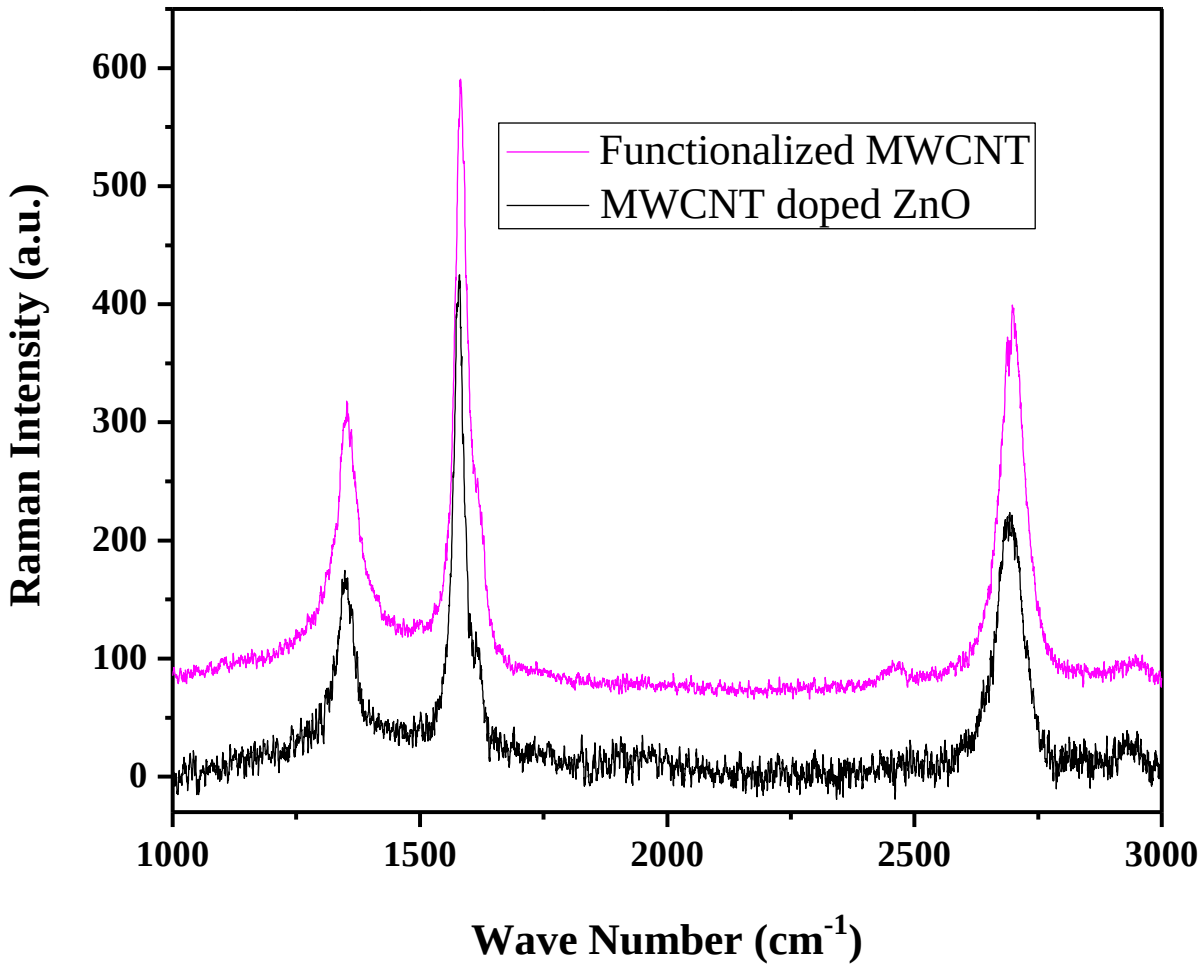
Raman Intensity (a.u.)
600
500
400
300
200
100
0
1000
1500
2000
2500
3000
Wave Number (cm-1)
Functionalized MWCNT
MWCNT doped ZnO

**Figure 3**

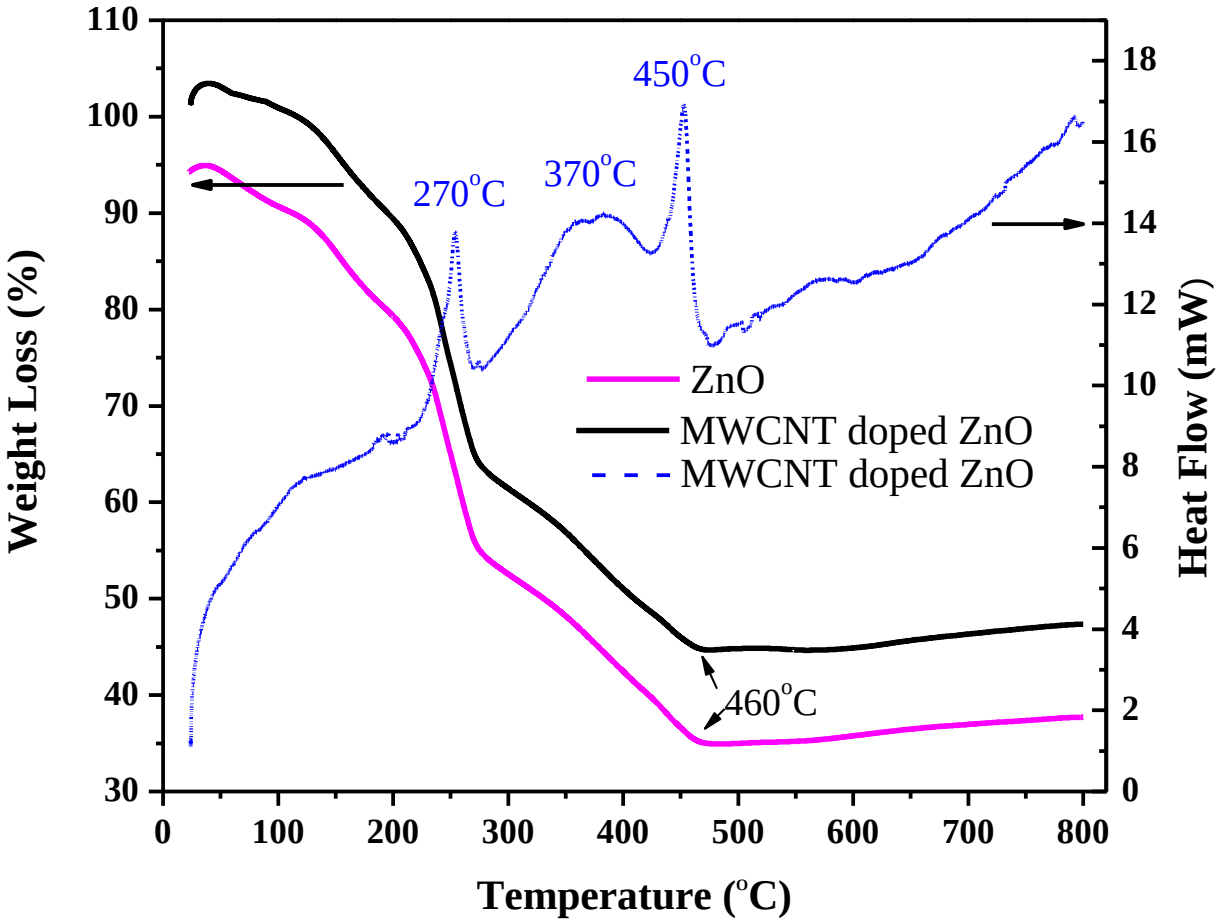
Weight Loss (%)
Heat Flow (mW)
Temperature (°C)
270°C
370°C
450°C
460°C
ZnO
MWCNT doped ZnO
MWCNT doped ZnO

**Figure 4**

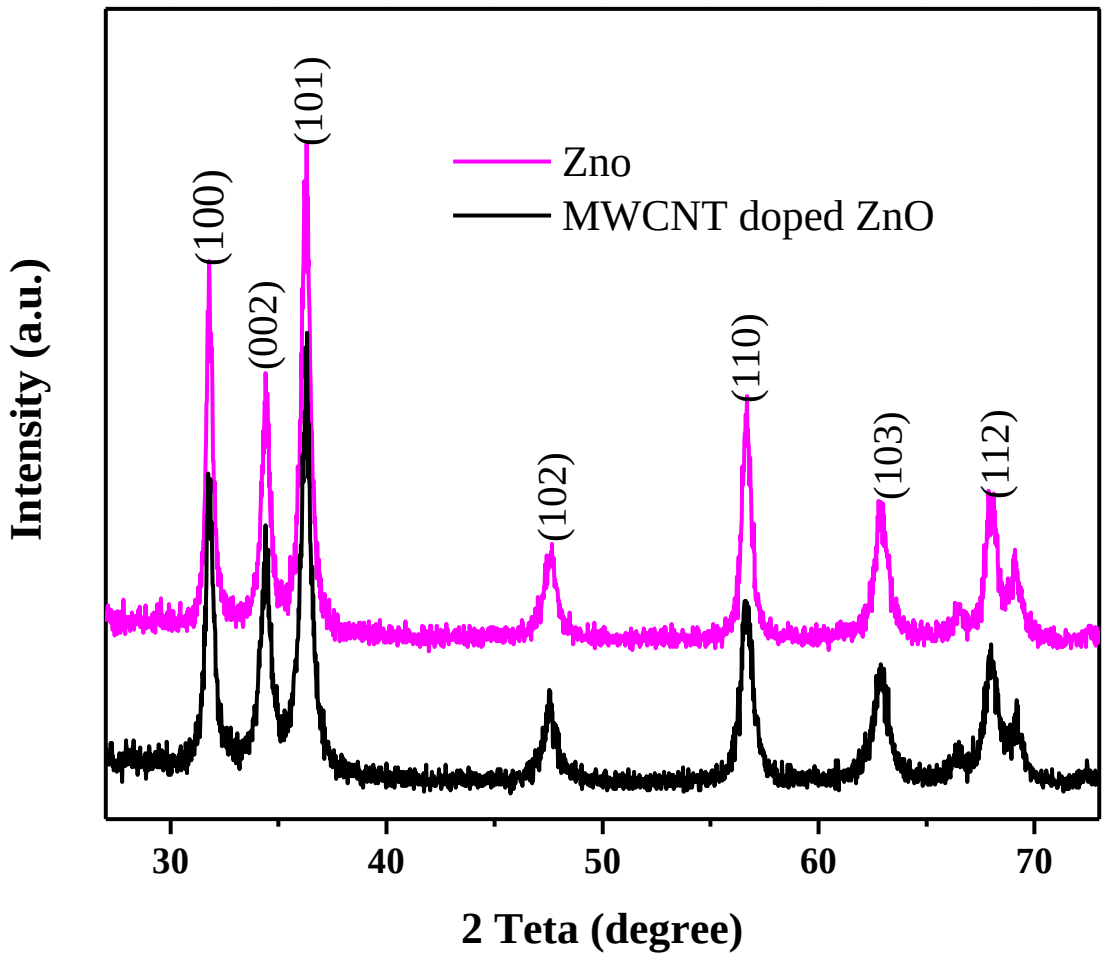
Zno
MWCNT doped ZnO
(100)
(002)
(101)
(102)
(110)
(103)
(112)
Intensity (a.u.)
30
40
50
60
70
2 Teta (degree)

**Figure 5**

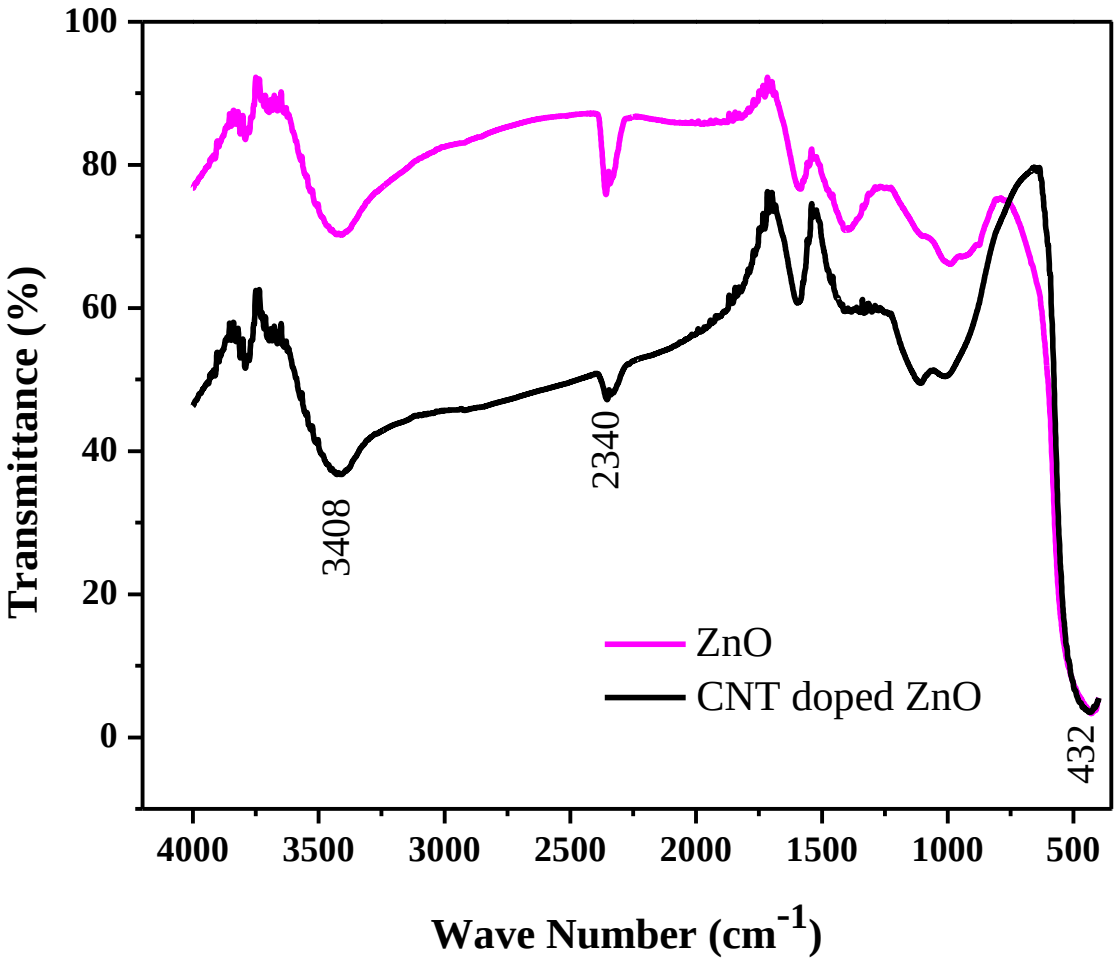
Transmittance (%)
100
80
60
40
20
0
4000
3500
3000
2500
2000
1500
1000
500
Wave Number (cm-1)
3408
2340
432
ZnO
CNT doped ZnO

**Figure 6**

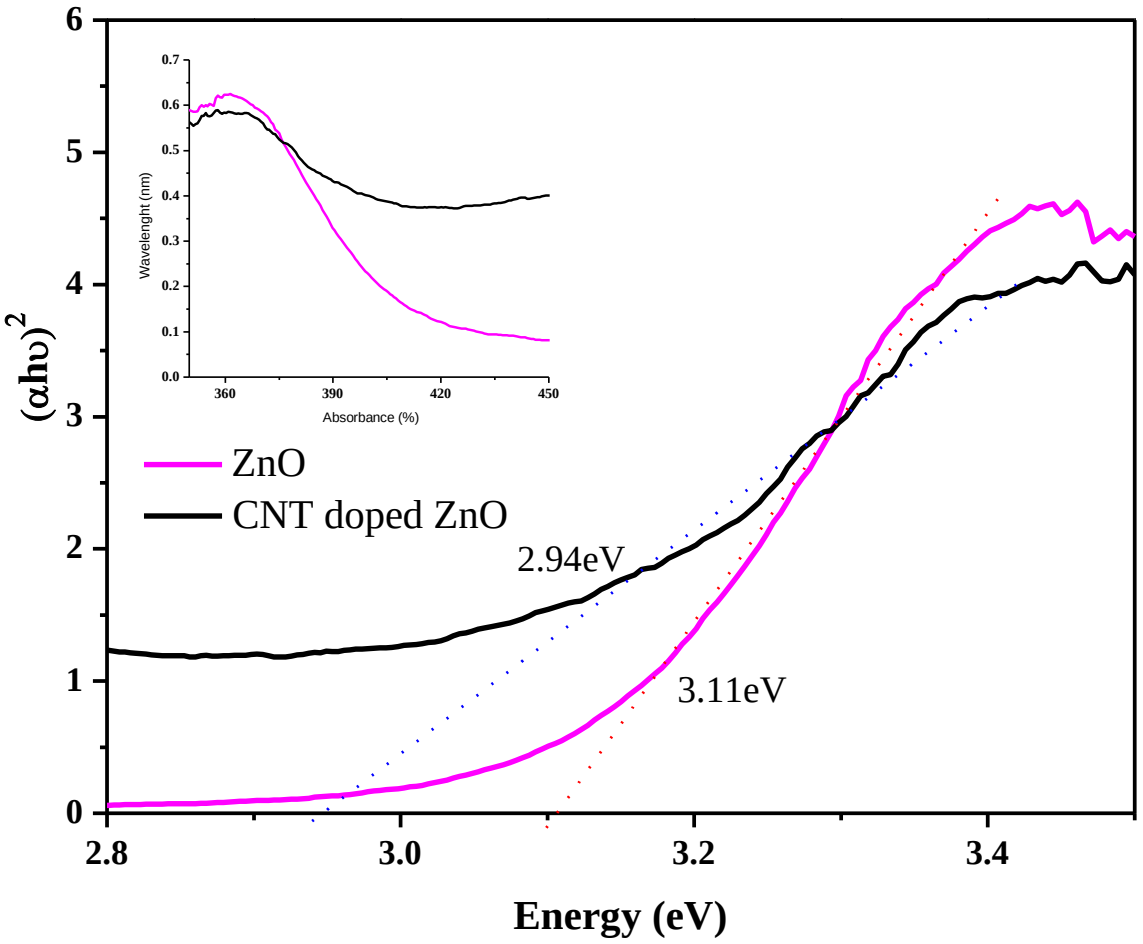
6
5
4
3
2
1
0
$(\alpha h\upsilon)^2$
2.8
3.0
3.2
3.4
Energy (eV)
ZnO
CNT doped ZnO
2.94eV
3.11eV
Wavelenght (nm)
Absorbance (%)
0.7
0.6
0.5
0.4
0.3
0.2
0.1
0.0
360
390
420
450

**Figure 7**

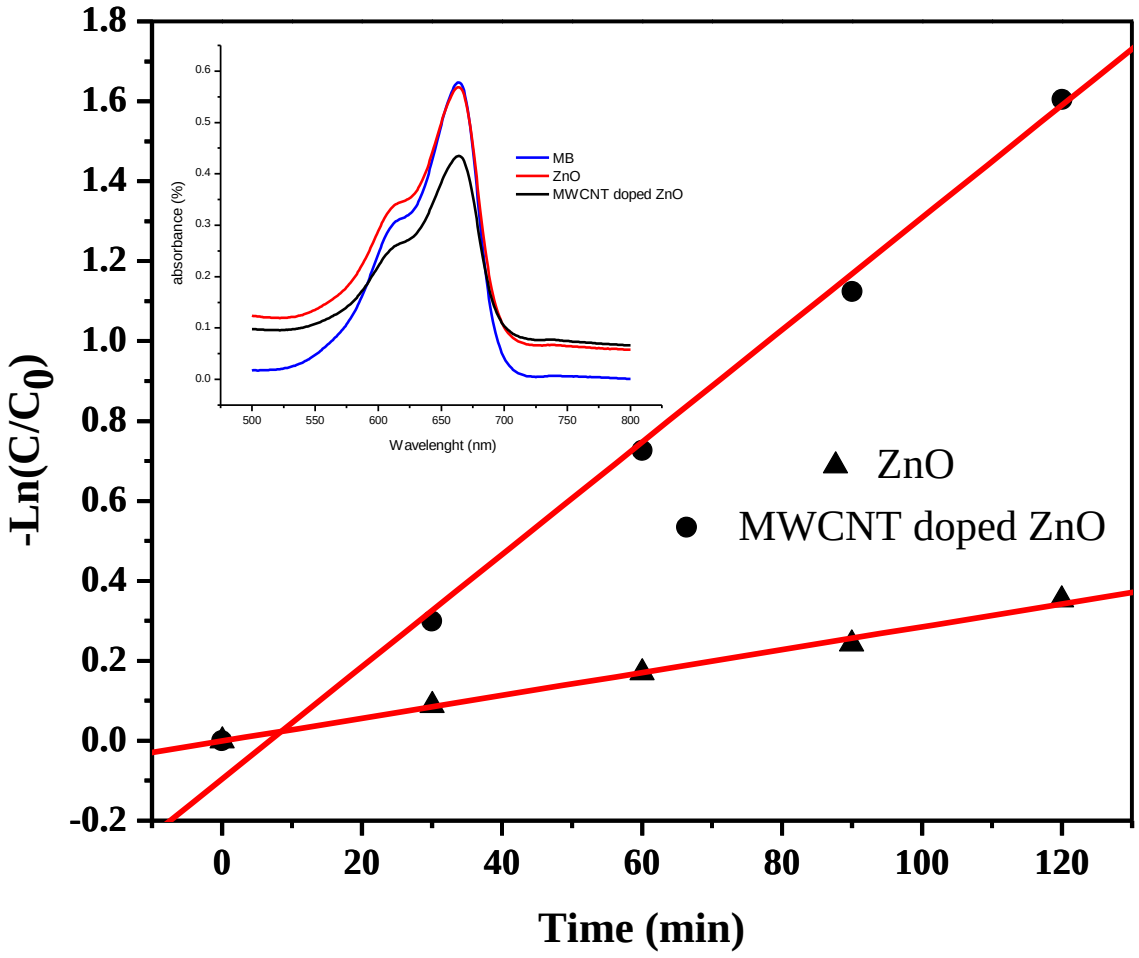
-Ln(C/C0)
Time (min)
ZnO
MWCNT doped ZnO
absorbance (%)
Wavelenght (nm)
MB
ZnO
MWCNT doped ZnO

**Figure 8**

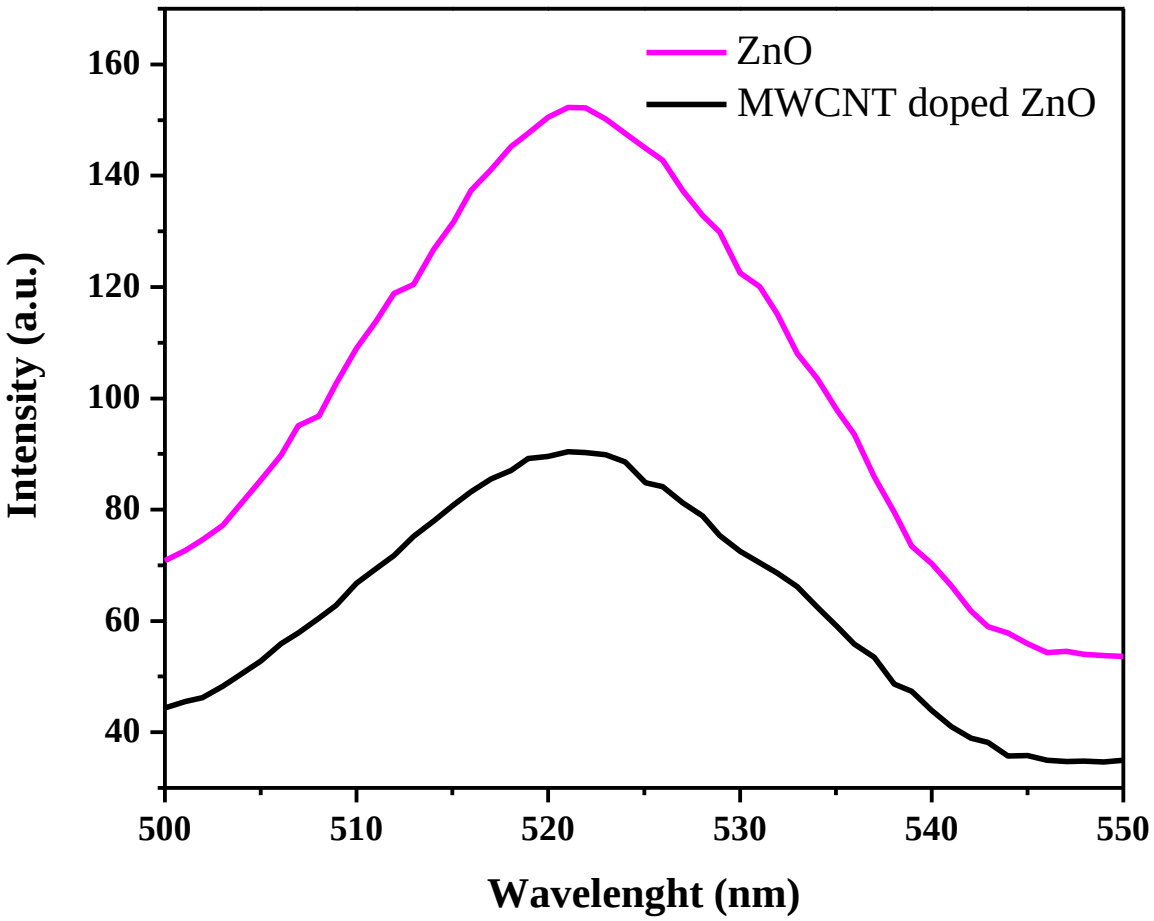
ZnO
MWCNT doped ZnO
Intensity (a.u.)
160
140
120
100
80
60
40
500
510
520
530
540
550
Wavelenght (nm)

**Figure 9**

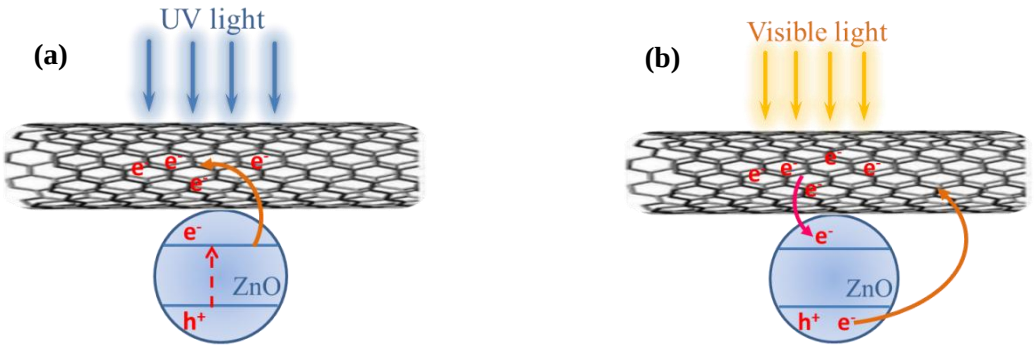

**Figure 10**